The Helios 1 compact superconducting storage ring X-ray source

by M. N. Wilson
A. I. C. Smith
V. C. Kempson
M. C. Townsend
J. C. Schouten
R. J. Anderson
A. R. Jorden
V. P. Suller
M. W. Poole

The basic properties of synchrotron radiation are described, the design of storage rings to produce synchrotron radiation is outlined, and the criteria for matching storage ring design to the needs of X-ray lithography are discussed. Simple scaling laws are presented showing the benefits for a storage ring of using the higher fields which superconducting magnets are able to provide. Helios 1 is a compact superconducting storage ring built by Oxford Instruments for installation at the IBM Advanced Lithography Facility (ALF). Design choices for superconducting rings are discussed, and the design and construction of Helios are described. Test results from the initial commissioning of Helios at Oxford are presented, but the main data on its performance when installed at ALF are given in another paper in this issue.

Introduction: Synchrotron radiation

Synchrotron radiation is the most powerful known continuous source of soft and hard X-rays. As such, it is well matched to the needs of production lithography. The Helios 1 compact synchrotron X-ray source, designed and built by Oxford Instruments with help from the UK Science and Engineering Research Council's Daresbury Laboratory, was installed at the IBM Advanced Lithography Facility (ALF) in 1991. It is now being used routinely in the development of X-ray lithography. **Figure 1** shows Helios 1 at Oxford, after completion of construction and before the start of its commissioning.

Like other kinds of electromagnetic radiation, synchrotron radiation is produced by the acceleration of electrical charge—in this case by using a magnetic field to make an electron beam follow a circular orbit. For electrons of energy E (MeV) in a field B (T), the orbit radius ρ (m) is

$$\rho \cong \frac{E}{300B}. \tag{1}$$

Figure 2 sketches the radiation emitted by a point charge traveling at velocity v and made to follow a circular orbit by the imposition of a magnetic field. At low values of v, the radiation follows a classical dipole pattern, but as v approaches the velocity of light c, the emitted radiation becomes sharply peaked in the forward direction [1, 2]. In fact, the opening angle ϕ of the radiation cone is given approximately by

$$\phi \cong \frac{1}{\gamma}, \tag{2}$$

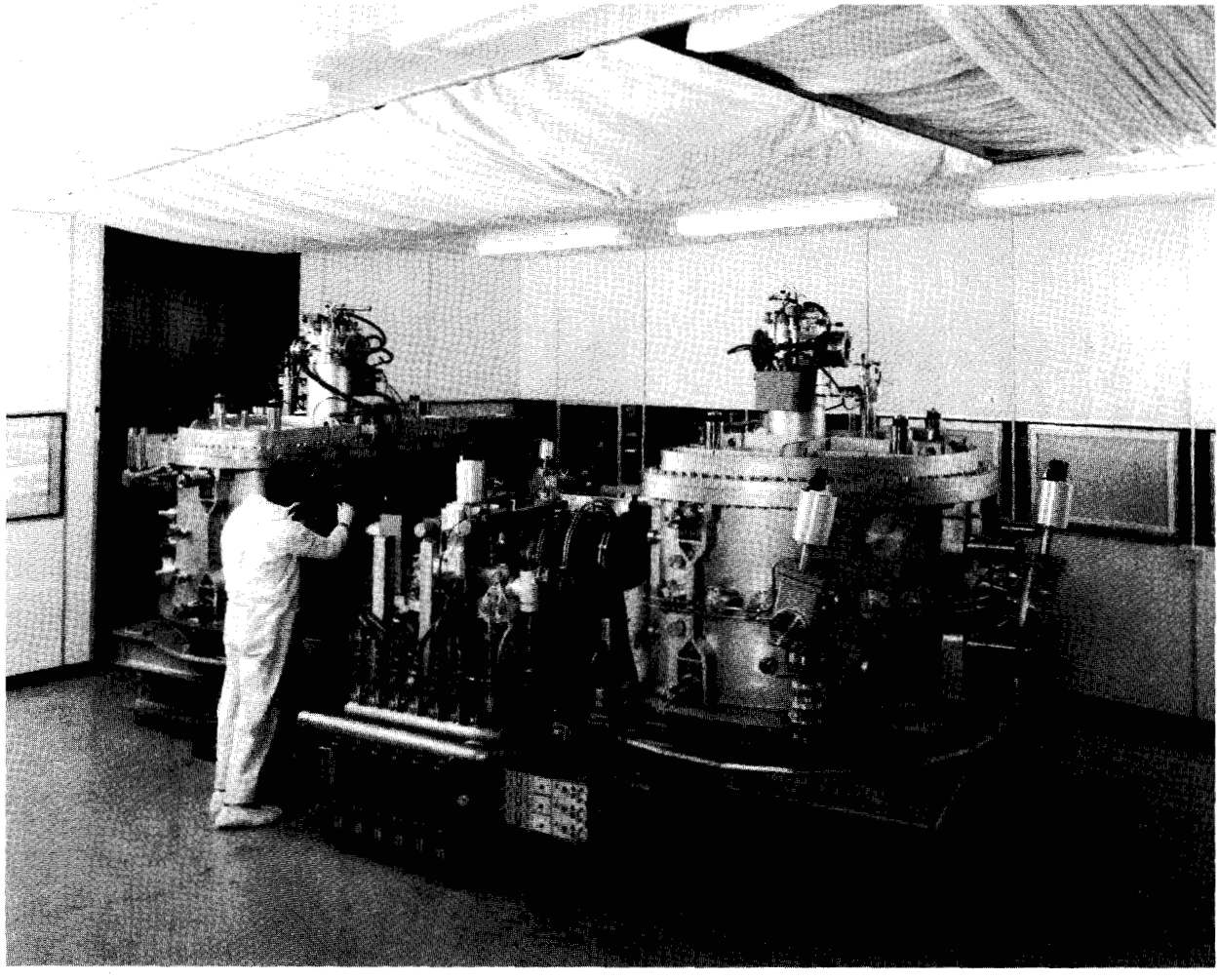

Figure 1

Helios 1 in the clean assembly area at Oxford, prior to being moved into the shielded enclosure for commissioning with electron beam.

where γ is the usual ratio of relativistic total energy to rest energy:

$$\gamma = \frac{E}{m_0 c^2} = \frac{E\ (\text{MeV})}{0.511}. \quad (3)$$

In the case where many electrons are traveling in a circular orbit, radiation is emitted in the form of a continuous fan with an opening angle ϕ. For soft X-ray emission we typically find that $\gamma \sim 1000$, so that the opening angle ϕ is ~1 mrad. This means that, at a distance of 10 meters from the circulating beam, the height of the emitted X-ray fan is only 10 mm.

The spectrum of the emitted X-rays follows a wavelength distribution not unlike that of black-body radiation. As the electron energy or magnetic field strength is increased, the wavelength distribution generally shifts downward, i.e., toward harder X-rays and more energetic photons. We look at this in more detail in a later section.

Storage ring X-ray sources

Because the circulating electrons radiate independently, the total emitted X-ray power is directly proportional to circulating current. Practical X-ray sources therefore seek to maximize this current by recirculating a beam in a closed loop—a storage ring. In such an arrangement, beams of electrons from an injection accelerator are successively "stacked" in the ring until circulating beams of a fraction of an ampere are attained.

Figure 3 illustrates the basic features of an electron storage ring. Beams of electrons from the linear accelerator (linac) are injected into a closed loop by the combined action of the pulsed kicker magnet and the

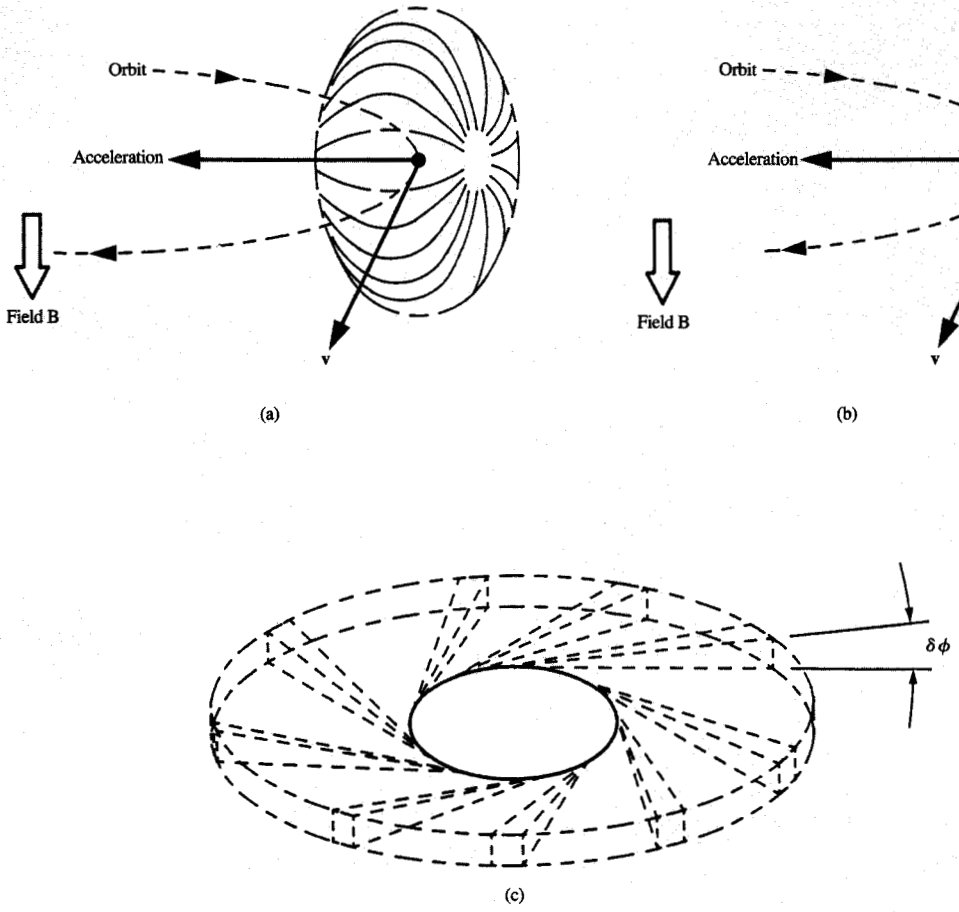

Figure 2

Synchrotron radiation emission from (a) a single electron at low velocity, (b) a single electron at high velocity, and (c) a circulating beam of electrons, producing a continuous radiation fan of vertical opening angle $\delta\phi$.

injection septum magnet. The closed loop is produced by a set of uniform field *dipole* magnets (in the example we show four). To confine a beam of finite size in closed orbit, one must also provide focusing in both transverse planes by means of gradient magnetic fields. Weak focusing in both vertical and horizontal planes may be provided by a weak gradient in the bending magnet field, i.e., a field whose value decreases slightly with increasing radius. In modern machines, however, it is more usual to use "strong focusing" produced by means of alternating gradients [3, 4]. Such gradients are produced by quadrupole magnets, which are often arranged in pairs with oppositely directed gradients. Each quadrupole produces a strong focusing effect in one plane and defocusing in the other, but the net effect on the particle beam is a focusing in both planes—the so-called principle of *alternating gradient focusing.* The imposition of these focusing fields causes the electrons to oscillate about their equilibrium orbit as they circulate around the ring: the so-called *betatron* oscillations. Stronger focusing produces correspondingly higher oscillation frequencies. The ratios between these transverse oscillation frequencies and the orbital revolution frequency are known as the horizontal and vertical betatron *tunes* of the ring.

Each time the beam traverses one of the bending magnets, it loses energy by emitting X-rays. In a typical ring, this energy loss amounts to tens or hundreds of keV per turn. If the stored beam is to be maintained in a steady

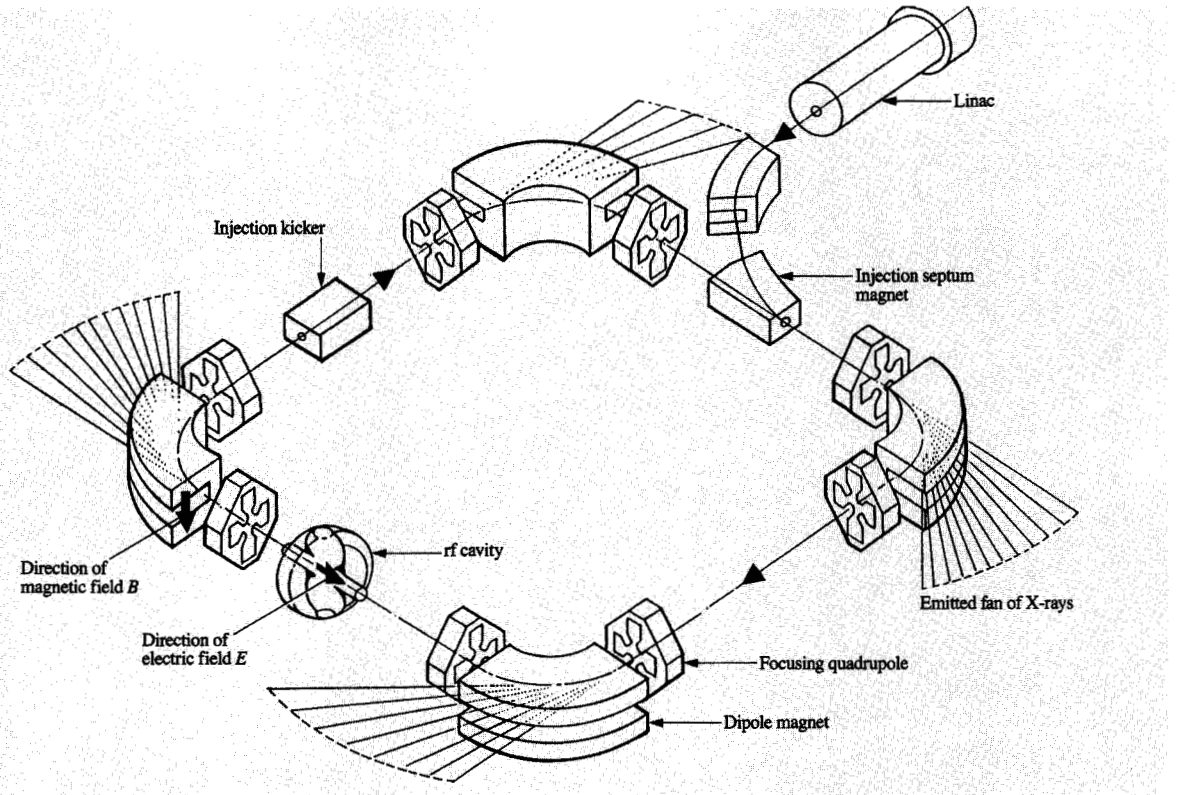

Figure 3

Schematic of a simple storage ring, showing how electrons are injected from the linac via the septum magnet, are bent into a closed loop by the four dipole magnets, focused by the quadrupole magnets, and accelerated by the rf cavity. Synchrotron radiation is emitted wherever the electrons are bent by the dipole magnets.

state, this loss must be replaced by means of an rf accelerating cavity. Such cavities generally operate at frequencies of 50–500 MHz, with voltages of hundreds of kV, which are somewhat greater than the energy loss per turn. In a ring which is correctly designed to provide the necessary *phase stability*, electrons automatically adjust their average phase such that they cross the cavity when the accelerating voltage is just what is required to make good the energy lost by X-ray emission. In fact, there exists a longitudinal phase focusing effect, with a corresponding oscillation frequency about the stable phase, which is closely analogous to the transverse focusing. The frequency of these oscillations in phase depends on the relationship between the energy lost per turn via X-ray emission and the cavity voltage.

As a result of the phase focusing effect, the electron beam divides itself into bunches of rather short duration. The maximum number of bunches that can be accommodated in the machine is just equal to the ratio of the cavity frequency to the orbit revolution frequency, often known as the harmonic number. In large machines, there are several hundred bunches; in compact rings there are just a few. These bunches give a nanosecond time structure to the emitted X-ray beam, which can be very useful in certain research applications but has no relevance to lithography.

The rf cavity also provides an ability to accelerate electrons within the ring. This facility is not always used; many rings inject beams at full energy and use the cavity only for replacement of X-ray losses. However, the injector accelerator needed to provide electrons at hundreds or thousands of MeV is a very expensive item, and there are good economic reasons for wishing to minimize the injection energy by performing part of the acceleration in the ring. In most rings, therefore, the beam is injected and stacked at some lower energy. The magnetic field is then ramped to its peak value, and electrons are accelerated to a higher energy by the combined action of the rf cavity and increasing magnetic

field. This action is the well-known process of synchrotron acceleration. Depending on a number of technical factors, synchrotron acceleration has been used to increase the beam energy in storage rings by factors between 3 and 40.

A typical operating cycle of the synchrotron/storage ring thus proceeds as follows. With the bending and focusing magnets set at their low-energy values, pulses of electrons from the injector are injected into closed orbit. Sufficient pulses are injected to stack the required circulating current, typically several hundred mA. During this process, the rf cavity is energized so that the circulating beam is divided into bunches. However, the energy loss per turn at this low energy is very small, and the bunches therefore adjust their phase to be near the zero crossing point of the rf cavity voltage so that they do not gain any net energy. When sufficient current has been accumulated at injection energy, fields in the bending and focusing magnets of the ring are ramped up to their full values over a period of a few minutes. Care must be taken to ramp the focusing magnets exactly in unison with each other and with the main dipole field, so that the "tune" of the machine remains constant during the ramp. During this process, the electrons adjust their phase at the cavity to gain exactly the right amount of energy needed to match the increasing field. When the desired energy is achieved, ramping ceases, and the stored beam continues to circulate at constant energy. Energy losses via X-ray emission are made good by energy inputs from the rf cavity. In effect, the circulating loop of electrons is behaving as a transducer which converts the rf power absorbed from the cavity into X-ray power emitted, with 100% efficiency.

X-rays matched to the needs of lithography

A detailed discussion of the relationship between the spectrum of X-rays emerging from the ring and the exposure process at the wafer is presented in [5]. Here we give only sufficient detail to permit a discussion of the optimum design of the storage ring.

The emission of X-ray photons by synchrotron radiation follows a universal law whereby the number of photons emitted per second per milliradian of bend within a frequency bandwidth of 0.1% is given [2] by

$$N(h\nu) = 1.256 \times 10^7 I\gamma G_1(y), \tag{4}$$

where $h\nu$ is the energy of the emitted photon, I is the circulating current in mA, and y is the ratio

$$y = \frac{h\nu}{h\nu_c}, \tag{5}$$

where $h\nu_c$ is defined as the critical photon energy for a given electron energy and bending field:

$$h\nu_c = \frac{3hc\gamma^3}{4\pi\rho} = \frac{2.22 \times 10^{-6}E^3}{\rho} = 59.8B^3\rho^2, \tag{6}$$

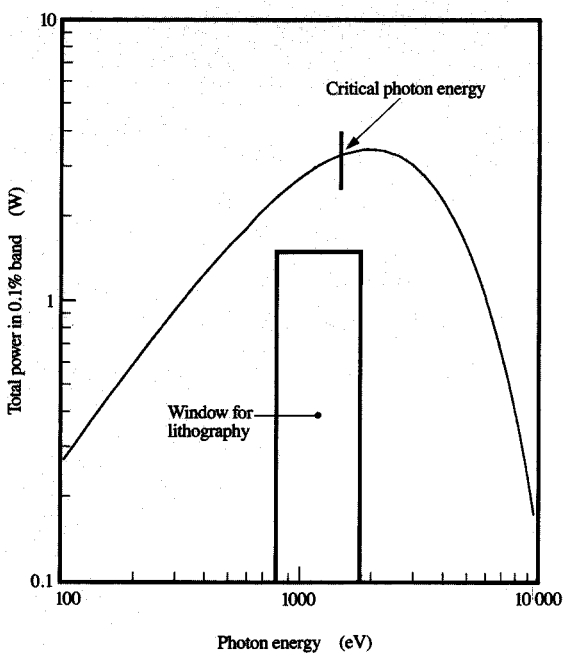

Figure 4

Power spectrum of the X-rays emitted by Helios 1, showing the window useful for lithography.

where $h\nu_c$ is in eV, E is in MeV, B in tesla, and ρ in m.

The function $G_1(y)$ is given by integrating a modified Bessel function of the second kind:

$$G_1(y) = y \int_y^\infty K_{5/3}(t)\, dt. \tag{7}$$

The power spectrum from the whole ring, in watts per 0.1% bandwidth, is thus given by

$$P(h\nu) = 1.256 \times 10^7 \times 1.602 \times 10^{-19} \times 2\pi \times 10^3 h\nu I\gamma G_1(y), \tag{8}$$

where the additional numerical factors are to convert photon energy (eV) to joules and to give total ring power over 2π radians.

Figure 4 plots the power spectrum of X-rays emitted by Helios, which has I = 200 mA, E = 700 MeV, and B = 4.5 T. Not all of this spectrum is useful for lithography. As discussed in [5, 6], softer radiation below about 800 eV is filtered out by the beryllium window at the end of the beamline and by the "transparent" silicon regions of the mask. Silicon also has an absorption edge at 1800 eV, which cuts off most of the radiation above 1800 eV. The

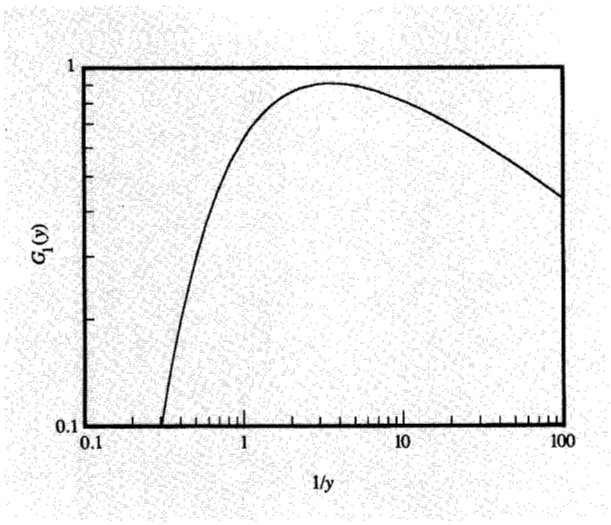

Figure 5

Function $G_1(y)$ versus $1/y = h\nu_c/h\nu$ showing a maximum at $1/y = 3.3$.

effective window for lithography thus lies between photon energies of 800 and 1800 eV, as shown in Figure 4. To calculate the exposure process exactly, it is necessary to track the emitted spectrum through each stage of the beamline, windows, mask, and resist. For design optimization of the storage ring, however, it is only necessary to maximize the radiated power in the 800–1800-eV window. This power may be calculated for Helios from **Figure 5** to be 2.4 kW, which may be compared with the total ring power output (at 200 mA) of 8.2 kW, calculated from

$$P_{\text{tot}} = 2.65 \times 10^{-5} IE^3 B. \tag{9}$$

For practical design purposes, one may get a good estimate (to ~2% of the exact value) of the power in the 800–1800-eV window via the approximation

$$P_{\text{window}} = P(1300 \text{ eV}) \times \frac{1000}{1300} \times 10^3. \tag{10}$$

To get the highest lithography power, it is therefore sufficient to maximize the ring output at 1300 eV. From Equation (8), it may be seen that this amounts to choosing the critical photon energy $h\nu_c$ such that G_1 is maximized. Figure 5 plots $G_1(y)$ against $1/y$; i.e., $h\nu_c/h\nu$, where we now regard $h\nu$ as fixed at 1300 eV and $h\nu_c$ as the variable. It may be seen that there is a broad optimum around $1/y = 3.3$; i.e., $h\nu_c = 4300$ eV. In practice, however, such a large "tail" of high-energy photons would be undesirable for lithography, and it is preferable to choose a lower critical energy. For Helios we chose $h\nu_c = 1470$ eV, which produces much less hard radiation, at the expense of ~23% reduction in the power at 1300 eV as compared with the optimum $h\nu_c$.

It is also common to characterize X-radiation by its wavelength:

$$\lambda = \frac{c}{\nu} = \frac{1241}{h\nu}. \tag{11}$$

Thus, for Helios we have a critical wavelength $\lambda_c = 0.84$ nm.

Scaling laws and the choice of magnetic field

For any storage ring, the critical wavelength is rather simply related to the magnetic field and bending radius by

$$\lambda_c = \frac{20.74}{\rho^2 B^3}. \tag{12}$$

It may thus be seen that, for a specified λ_c, the radius of bending ρ scales as $B^{-3/2}$. This scaling is the main argument for the use of superconducting magnets, which are able to produce much higher fields than conventional iron magnets.

In addition, the magnetic field has an important effect on the injection process because it affects the damping of betatron oscillations in the circulating beam. We see in a later section how this damping determines the repetition rate for injection: Stronger damping allows faster injection. Strong damping can also be very useful in suppressing potentially disruptive instabilities during the injection process. Oscillations of the electrons in all three planes are damped by energy losses via synchrotron radiation. Damping in the vertical direction is the simplest to formulate analytically; damping in the horizontal and longitudinal planes may then be obtained from it via a numerical factor, which depends on the magnetic field shape and is independent of energy [7]. From [7], the vertical damping time is

$$\tau_z = \frac{2E_i t}{U}, \tag{13}$$

where E_i is the injection energy, t is the orbit revolution time, and U is the energy loss (MeV) per turn via synchrotron radiation [7],

$$U = \frac{8.85 \times 10^{-14} E_i^4}{\rho}. \tag{14}$$

The bending magnets normally occupy some fraction m of the orbit perimeter, with the remainder being taken up by rf cavity, focusing magnets, injection magnets, etc. The orbit revolution time t is therefore $2\pi\rho/mc$, where c is the velocity of light. Eliminating ρ from Equations (6), (13), and (14), we find

$$E_i = \frac{19.9}{B}\left\{\frac{h\nu_c}{\tau_z m}\right\}^{1/3}. \quad (15)$$

Thus, for a fixed critical photon energy (defined by the needs of lithography), a fixed damping time (defined by the injection process), and a fixed m (defined by the layout of the ring), the injection energy is inversely proportional to the maximum field in the bending magnets.

Conventional bending magnets use a soft iron yoke, which is magnetized by currents circulating in copper windings. Their maximum field is limited to ~2 tesla by saturation in the iron. Nonlinearities become significant at lower fields, however, and these cause errors in the field shape. At a single fixed field, these errors may be compensated by suitable shaping of the iron, but errors occurring as the field is ramped are difficult to correct over the entire range of the ramp, and they effectively limit the accurate field to a maximum value of about 1.6 T. A further complication in electron storage rings is the need for a gap in the iron yoke to let out the X-rays, the so-called C-magnet configuration. Because of their asymmetry, iron C-magnets are even more prone to saturation errors and are limited to fields of ~1.3–1.4 T.

Superconducting magnets are ultimately limited by the upper critical field of the superconducting material used. Although these fields can be very high in the brittle intermetallic compounds such as Nb_3Sn and even higher in the new high-temperature oxides, the mechanical properties of these materials render them unsuitable for the difficult winding configuration of a storage ring magnet. One is therefore left with the standard "workhorse" of superconducting magnets, the ductile alloy NbTi, which has a critical field of 11.4 T at the usual operating temperature of 4.2 K. Simple windings such as solenoid magnets can approach this upper limit quite closely, say ~9.5 T, but it is difficult to do better than ~6.5 T in the more complicated transverse field configuration needed for a storage ring. Here again, the need for an X-ray exit slot adds a further complication which effectively reduces the maximum field to ~5 T. For Helios we chose a field of 4.5 T in the electron beam aperture, which actually gives a peak field of 5.4 T on the superconducting winding.

Table 1 summarizes the effect of scaling laws by comparing a superconducting and a conventional ring, both of which are designed for the same critical photon energy λ_c. For the superconducting ring, we take the values of field B and circumference ratio m which were chosen for Helios. For the normal ring we take $B = 1.4$ T and $m = 0.5$ as being typical of many rings now in operation. To produce the same critical photon energy, the normal ring has a bending radius approximately six times that of the superconducting ring [see Equation (12)], allowing the latter to be much smaller. This compactness has benefits in a wafer fabrication facility, where space is expensive. It also allows the ring to be transported intact, which means that it can be assembled and commissioned at the vendor's factory and then shipped to the user site as a fully tested working unit.

Table 1 Ring parameters with superconducting and normal magnets.

	Superconducting	*Normal*
Critical photon energy $h\nu_c$	1470 eV	1470 eV
Critical wavelength λ_c	0.84 nm	0.84 nm
Max bending field B	4.5 T	1.4 T
Bending radius R	0.52 m	3.0 m
Circumference ratio m	0.34	0.5
Circumference C	9.6 m	37.7 m
Max electron energy E	700 MeV	1260 MeV
Injection energy at $\tau_z = 0.047$ s	200 MeV	567 MeV
Injection energy at $\tau_z = 0.375$ s	100 MeV	283 MeV

The damping times τ_z at injection listed in Table 1 correspond to the injection energies of 200 MeV and 100 MeV chosen for Helios 1 and Helios 2, respectively (Helios 2 is the second ring of the series, now under construction at Oxford). We discuss this different choice of energy in the next section. It may be seen that to obtain the same damping times in a normal ring requires an injection energy which is approximately two and one half times greater. The superconducting ring thus brings considerable savings in the cost of the injector. Furthermore, the cost of shielding is also reduced, because the greatest loss of electrons occurs during the injection process and these electrons produce harmful gamma rays plus neutrons, which must be shielded. The required shield thickness decreases as the electron energy is reduced.

Some design options

Having made the basic choice of bending field magnitude, one must then make several other design choices. First, it is necessary to decide how the bending magnets are to be arranged. If they are to be superconducting, it is generally preferable to choose a small number of large units rather than vice versa, because the leakage of heat into cryogenic equipment increases with surface area. As sketched in **Figure 6**, the smallest number of magnets is obviously one, a circular ring with no straight sections. This arrangement, which has been adopted by Sumitomo Heavy Industries for their Aurora ring, has the advantage of compactness and a low cryogenic heat load. However, it does force the designer to fit all of the ring components, such as injection, rf cavity, and diagnostics, within the aperture of the magnet; such arrangements can be very congested. For this reason, we have adopted the two-sector racetrack

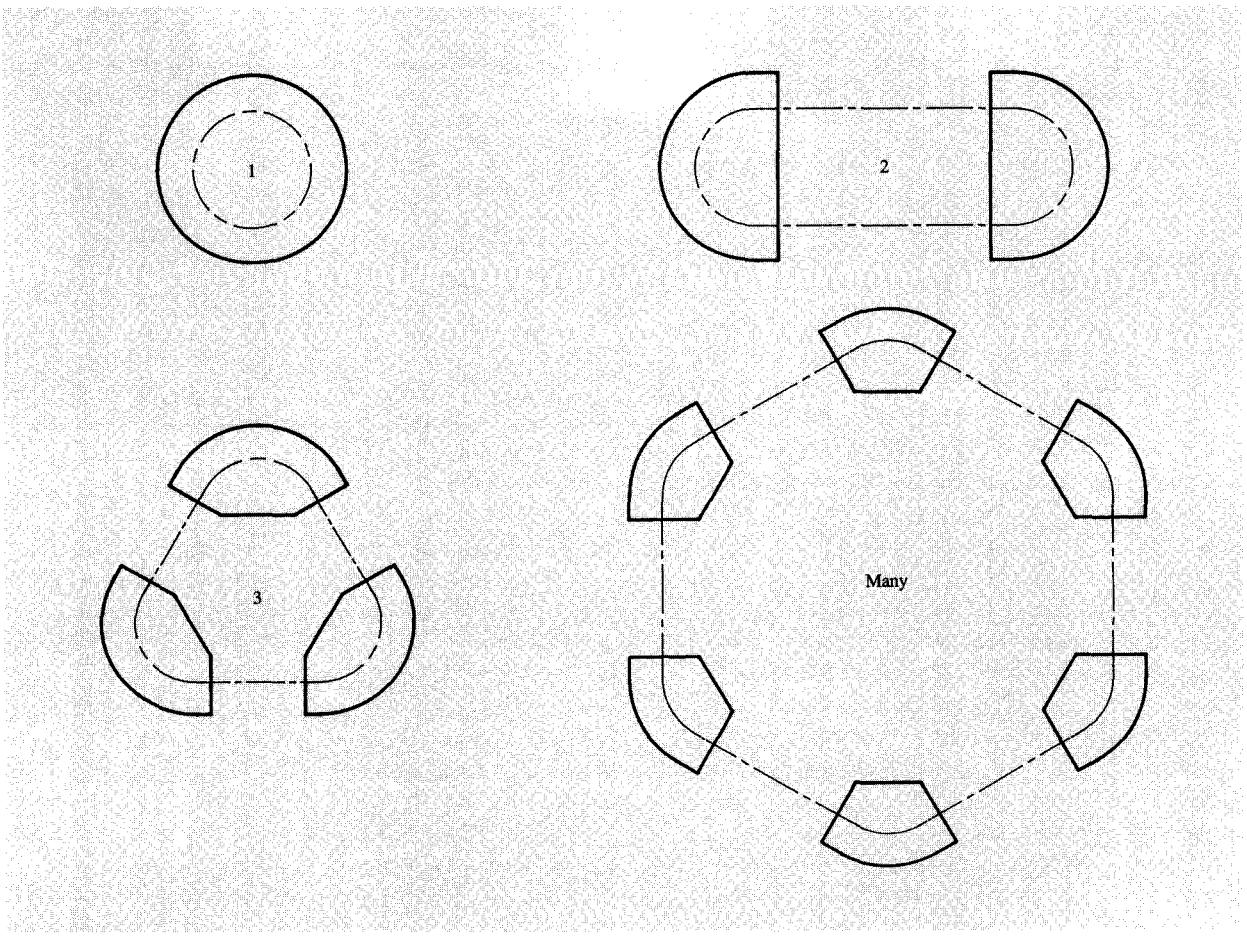

Figure 6

Possible storage ring designs with different numbers of magnets.

style for Helios, and a similar layout has been used in several other compact rings [8]. In this arrangement, the injection-pulsed magnets, rf cavity, quadrupole magnets, correction magnets, and diagnostics can all be located in the two straight sections, leaving the two dipoles quite clear. Of course, it is also possible to divide the ring into many more sectors, as sketched in Figure 6. Such arrangements are commonly used in conventional rings for research, where it is desirable to have many straight sections for special insertion devices and where the large number of focusing magnets may be used to produce a small beam size, but they have no advantage in lithography rings.

A choice for the superconducting magnets themselves is whether to use iron. Iron yokes, which are always used in conventional magnets, are often used with superconducting accelerator magnets to shape the field, reduce the required magnetizing current, and screen the fringe field. At high fields, however, the iron is driven deeply into saturation, producing nonlinear effects and consequent field errors when the magnet is ramped from injection energy up to final energy. These errors can cause loss of beam during the ramp; they can be offset somewhat by correction windings, but on Helios we decided to avoid the problem entirely by using no iron. As a consequence, the fringe field from the bending magnets is appreciable but, given that personnel must always be excluded from the shielded enclosure during ring operation, this fringe field is of little consequence. A serious disadvantage of iron magnets is their considerable weight, which makes transportation and installation difficult.

Given that the superconducting magnet must be cooled to ~4 K for operation, one has the option of using this cold surface to improve the vacuum quality. Vacuum is important in storage rings because it is usually the dominant factor in determining the lifetime of the stored

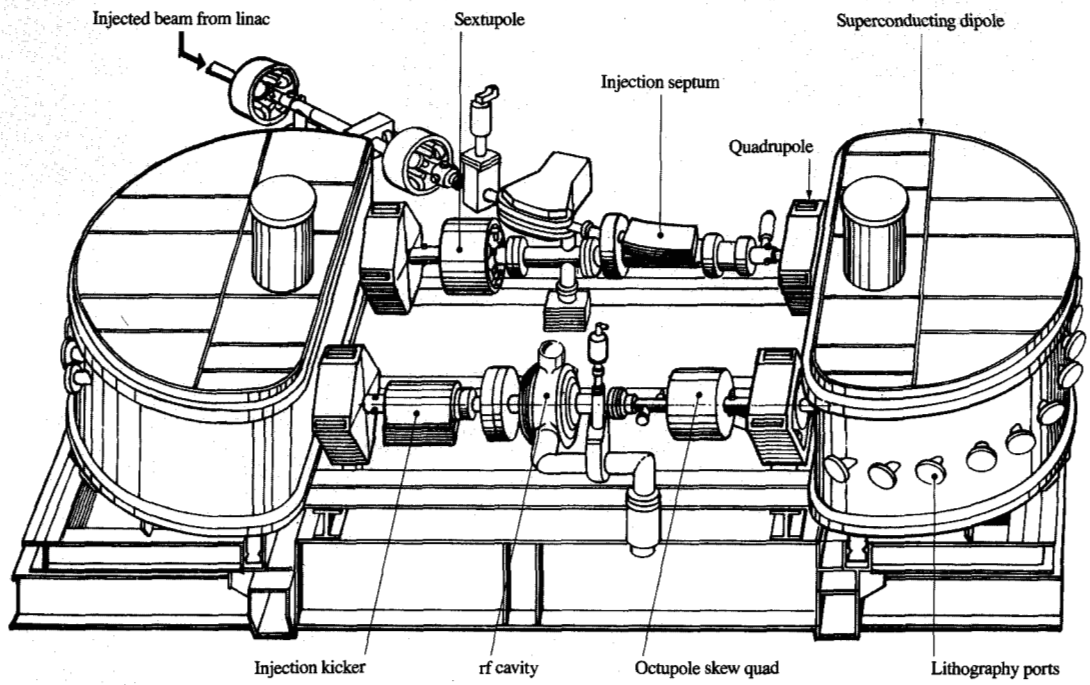

Figure 7

Helios 1: a simplified artist's impression of the ring.

beam. Unfortunately, the beam itself tends to spoil the vacuum because the emitted X-rays cause photodesorption from surfaces within the vacuum chamber. Naturally this problem is worst around the bending magnets where the X-rays are emitted. By using the cold helium vessel as the wall of the electron beam pipe, one can ensure that molecules which are desorbed by the emitted X-rays will be condensed on the cold surfaces before they can reach the electron beam. This arrangement is the one adopted for Helios and is without doubt a contributing factor to the excellent beam lifetimes which have been achieved [9]. The main disadvantage of cold bore is that it becomes necessary to warm up the magnet if the ring must be vented, thereby introducing some delay. But with careful operating procedures and a well-designed system of fast shut-off valves for the X-ray beamlines, the need for such venting should be very infrequent.

The design of Helios

- *Focusing and stability*

Figure 7 shows an artist's impression of Helios, simplified to bring out the salient features. It is a two-sector racetrack ring with two 180° superconducting dipole (bending) magnets. Focusing for the circulating electrons is provided by the combined effects of four conventional iron quadrupole magnets and a gradient in the dipole field. The quadrupoles produce a focusing effect in the horizontal plane but a defocusing effect in the vertical direction. This effect is countered by vertical focusing effects in the gradient dipole, so that the sum total around the ring is one of focusing in both planes simultaneously.

As noted earlier, the ratio of betatron frequency to the frequency of revolution (i.e., the number of transverse oscillations per orbit) is known as the betatron tune of the ring. In Helios we have arranged for the horizontal and vertical betatron tunes to be close to 1.5 and 0.5, respectively. However, it is important to avoid integer or low-order fractional values of tune because the resulting resonances cause loss of beam. For example, a vertical tune of 0.5 means that a vertical betatron oscillation returns to exactly the same phase after every second revolution; thus, small errors grow without limit via a kind of positive feedback effect, and the beam is lost.

In addition to simple resonances within a plane, there are others which couple motion from one transverse plane

Table 2 Key parameters of Helios 1.

		Specified	*Achieved to date*
Electron energy		E = 700 MeV	700 MeV
Dipole (bending) field		B_0 = 4.50 T	4.50 T
Stored electron beam:			
at injection energy		I = 200 mA	540 mA
at full energy		I = 200 mA	297 mA
Bending radius		R_0 = 0.519 m	0.519 m
X-ray total emitted power		P = 8.2 kW	11.2 kW
Energy loss per turn		U_0 = 40.9 keV	40.9 keV
Max source size (Gaussian)	radial	σ_r = 1.5 mm	= 0.4 to 1.2 mm
	vertical	σ_v = 1.1 mm	= 0.2 to 0.6 mm
Total divergence (Gaussian)	radial	$\sigma_{r'}$ = 3.2 mrad	not measured
	vertical	$\sigma_{v'}$ = 0.7 mrad	= 0.4 to 0.6 mrad
rf frequency		f = 499.7 MHz	499.7 MHz
Harmonic number		h = 16	16
Base pressure		5×10^{-10} torr (6.7×10^{-8} Pa)	3×10^{-10} torr (4×10^{-8} Pa)
Operating pressure		3×10^{-9} torr (4×10^{-7} Pa)	1×10^{-9} torr (1.33×10^{-7} Pa)
Beam lifetime at 200 mA		$t > 5$ hr	19 hr
Injection energy		E = 200 MeV	200 MeV
Injection source		linac	linac
Injection current		10 mA	20 mA
Injection pulse length		120 nS	120 nS

to another or to motion in the longitudinal direction via oscillations about the synchronous phase of the rf cavity. In the longitudinal direction, the frequency of oscillation about the synchronous phase is known as the synchrotron frequency, and the ratio of this frequency to the revolution frequency is the synchrotron tune. The global condition for a coupling resonance among motions in all three directions is given by

$$nv + mh + qs = p, \tag{16}$$

where v and h are the vertical and horizontal betatron tunes, s is the synchrotron tune, and n, m, q, and p are integers. Successful operation of the ring depends on steering a well-judged course among these resonances, for which it is necessary to have the ability to vary the tune in all three planes independently. In Helios the betatron tunes in each horizontal plane may be adjusted by changing the gradients of the four conventional quadrupoles (changing in unison) and the dipole gradient, which is adjusted by special superconducting quadrupole trim windings within the dipole. Synchrotron tune is adjusted by changing the rf cavity voltage.

The resonant instabilities discussed thus far are all caused by interactions between individual electrons and the externally applied magnetic focusing and bending fields. In addition, the electron beam can suffer from collective instabilities, which are caused by different electron bunches or different parts of the same bunch interacting with one another via the electromagnetic structures in the ring. The higher-order electromagnetic modes (HOMs) of the rf cavity are generally the most serious concern in this regard. It is sometimes useful to picture such a collective instability as transferring some of the stored electromagnetic energy in the rf cavity to longitudinal and transverse electron beam motion. Successful operation of the ring depends on raising the beam current threshold for the onset of these instabilities, for example by altering the betatron and synchrotron tunes or by changing the HOM spectrum of the rf cavity. Alternatively, additional damping may be introduced to supplement that already coming from synchrotron radiation emission. One method is to introduce an octupole component in the magnetic field; the Helios straight section contains a single conventional octupole magnet for this purpose.

One common form of collective instability is caused by *chromaticity* in the ring. From Equation (1), the bending power of a given field is inversely proportional to energy. Thus, the focusing power of the quadrupoles, and hence the tune of the ring, also varies with electron energy. It follows that a spread of energy within the beam gives rise to a spread of tune. By analogy with optics, this effect

is known as chromaticity. Excessive chromaticity can lead to collective instabilities and must be compensated by sextupole magnets, in which the gradient increases linearly with distance from the equilibrium orbit. Chromaticity in each plane must be compensated separately, requiring two independent sextupoles. In Helios, one conventional sextupole is located in a straight section and four others, acting in unison, are located at the ends of the dipoles. **Table 2** lists the main parameters of Helios 1.

• *Injection*

Electrons for injection into Helios are provided by a linac built by CGRMeV of Buc France [10]. The linac produces pulses of electrons at 200 MeV with an instantaneous current of 10–20 mA. It is therefore necessary to inject many pulses in order to accumulate the desired circulating current of 200–300 mA.

Figure 8 shows a schematic of the linac and injection beam transfer line. Electrons, produced in a triode gun whose cathode is at −50 kV, are passed to a *prebuncher* cavity which modulates the beam at 500 MHz so that its time structure is matched to that of the ring rf cavity. Further modulation at 3 GHz is then applied by the *buncher*, to produce a second time structure matched to the operating frequency of the linac. The beam then enters the first of two accelerating sections in the form of disc-loaded waveguides, each of which is energized at 3 GHz by a 35-MW Thomson klystron to produce a forward-traveling electromagnetic wave. Electrons ride on the crest of this electromagnetic wave, gaining energy as they go and acquiring in total ~100 MeV per section. To reduce energy dissipation, the klystrons are powered in short bursts of a few ms duration, with a repetition rate of 10 Hz.

Because linear accelerators tend to produce a fairly large energy spread, it is necessary to measure and filter the beam before passing it to the ring. This is carried out at the start of the injection transfer line which, as shown in Figure 8, is arranged in the form of an energy spectrometer. On leaving the linac, the electron beam is focused by a quadrupole doublet and is then bent by a dipole magnet which spreads electrons of different energies across a plane downstream from the dipole. Using a slit at this plane, the off-energy electrons are filtered out, and a beam of correct energy (±0.5%) is transmitted to the ring via the second bending magnet and more quadrupoles. The downstream section of the beam transfer line is designed to be *achromatic*, so that when the beam eventually arrives at the ring, all electrons within the ±0.5% energy band are focused at the same point.

On arrival at the ring, electrons are turned parallel to the orbit by the *septum magnet*. As its name implies, this magnet makes use of a thin current-carrying sheet or septum in such a way as to produce field on one side of the septum and zero field on the other. Beam from the linac is deflected by the septum field, while beam circulating in the ring, which is on the other side of the septum, is not. The Helios septum magnet is pulsed in synchronism with the linac pulse, and the septum itself takes the form of a passive eddy current shield.

To ensure that the injected beam joins onto the beam already circulating in the ring, it is necessary to apply a

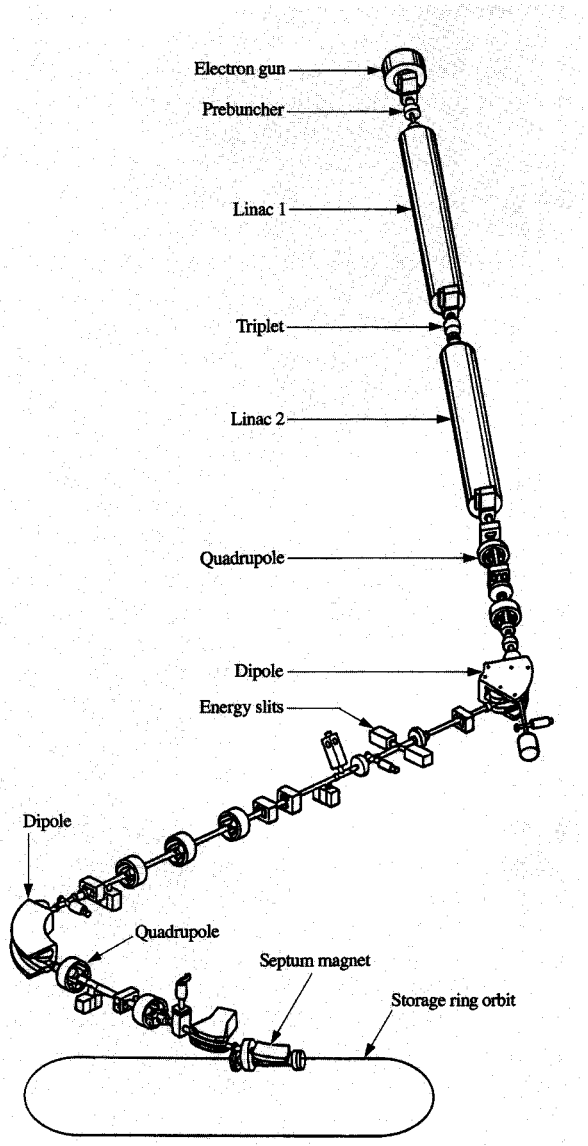

Figure 8

Schematic of the Helios 1 injection linac and transfer line.

perturbation to the circulating beam. This is done by the kicker magnet which, as shown in Figure 7, is located in the straight section opposite the septum. The kicker produces a pulse of field which deflects the circulating beam toward the septum. Beam injected through the septum is now rather close to the circulating beam, and oscillates about the circulating beam at the betatron frequency. Given a suitable choice of betatron tune, these oscillations can be arranged such that the newly injected beam will miss the septum for several revolutions, but eventually the oscillations must arrive again at their point of entry, and hit the septum. However, if the kicker is switched off just before this happens, all of the beam is moved away from the septum, and the newly injected beam then continues to oscillate about the stored beam indefinitely. Now we see the importance of the damping time mentioned earlier, because pulsing the kicker again would merely drive the oscillating part of the beam into the septum. If, however, one waits until the oscillations have died away via synchrotron radiation damping, the injection process may be repeated without hitting the septum. Damping thus determines the repetition rate of the injection process. For Helios 1, with a repetition rate of 5 Hz, the required damping time is a fraction of a second.

We have also noted that damping helps to suppress any destructive instabilities which might be excited by the injection process, and such considerations are usually a stronger factor in the choice of damping time than the achievement of a given repetition rate. Indeed, it was a fear of such instabilities which prompted the choice of 200 MeV as the injection energy for Helios 1, giving a vertical damping time of 0.047 s (Table 1). The closely related radial damping time is 0.07 s, which is clearly much shorter than required for the design injection rate of 5 Hz. By experimentation on Helios 1, however, we have actually found that satisfactory injection can be achieved at 100 MeV, which according to Equations (13) and (14) implies damping times eight times greater. The next ring, Helios 2, now under construction at Oxford, will therefore be injected at 100 MeV.

- *The rf system*

The rf cavity may be seen in Figure 7 next to the kicker. It runs at 500 MHz, is somewhat spherical in shape, and is a close copy of the well-proven Daresbury SRS cavity. The rf power is provided by a more or less standard 60-kW TV transmitter (built by Comark Inc. using an EEV K3672BCD klystron) and is fed to the cavity via a coaxial line. The line is connected to a short section of WR1800 waveguide which communicates with the cavity via a ceramic window. Inside the waveguide are filters to absorb higher-order modes and the *matcher*, which is a movable element located within a shorted stub section of the waveguide. The matcher's main function is to minimize the power reflected back from the cavity to the transmitter, where it could damage the klystron. Because reflected power is a function of beam current and energy, the matcher must be controlled dynamically [11].

A second parameter which must also be controlled is the cavity resonant frequency, or *tuning*, which is varied by moving a noncontacting plunger located in a sidearm of the cavity. Ideally, the tuning should be adjusted so that the cavity and beam together behave as a purely resistive load; i.e., no power is reflected back to the klystron. However, the strong interaction between cavity and beam can produce certain types of instability which must be countered by detuning the cavity somewhat. Because the effective cavity impedance is affected by the beam, adjustment of cavity tuning must also be made dynamically by the control system, taking account of beam current and energy.

A typical cavity voltage setting at injection is ~80 kV, rising steadily during the ramp to ~220 kV at full energy. If the latter voltage is compared with the energy loss per turn of 40 keV at full energy, it is apparent that the cavity is running at much higher voltage than needed to make good the energy lost via synchrotron radiation. As noted earlier, phase stability ensures that the electron bunches adjust their phase so as to cross the cavity at just the right time to acquire the 40 keV lost. However, a higher cavity voltage is still needed to create a deep longitudinal potential well for the beam, thereby reducing the effects of intrabeam (Touschek) scattering [12] and quantum losses [7], which would otherwise reduce the lifetime of the stored beam.

- *Superconducting dipoles*

The superconducting dipole magnets are the main innovative feature of Helios and were the subject of an extensive development program at Oxford. They provide a field of 4.5 T, with a fixed gradient in the radial direction of $-1.8\ \mathrm{Tm}^{-1}$ over a 180° arc; this field is accurate to $\sim 5 \times 10^{-4}$. In addition, several trim coils are provided to introduce variable components of quadrupole, sextupole, and radial field.

As noted earlier, after a careful evaluation of the alternatives, we chose a cold-bore design with no iron. **Figure 9** shows a cross section of the coils in their liquid helium cryostat. The main field is provided by a set of four coils of rectangular cross section, located symmetrically above and below the beam plane. Rectangular coils were chosen in preference to the more exotic "cos θ" cross sections used for magnets at the large superconducting rings such as Fermilab, because here we need to bend the coils through a 180° arc—and this is very difficult with coils of irregular section. Nevertheless, by careful optimization of the relative sizes, shapes, and positions of just four rectangular coils (two above and two below the

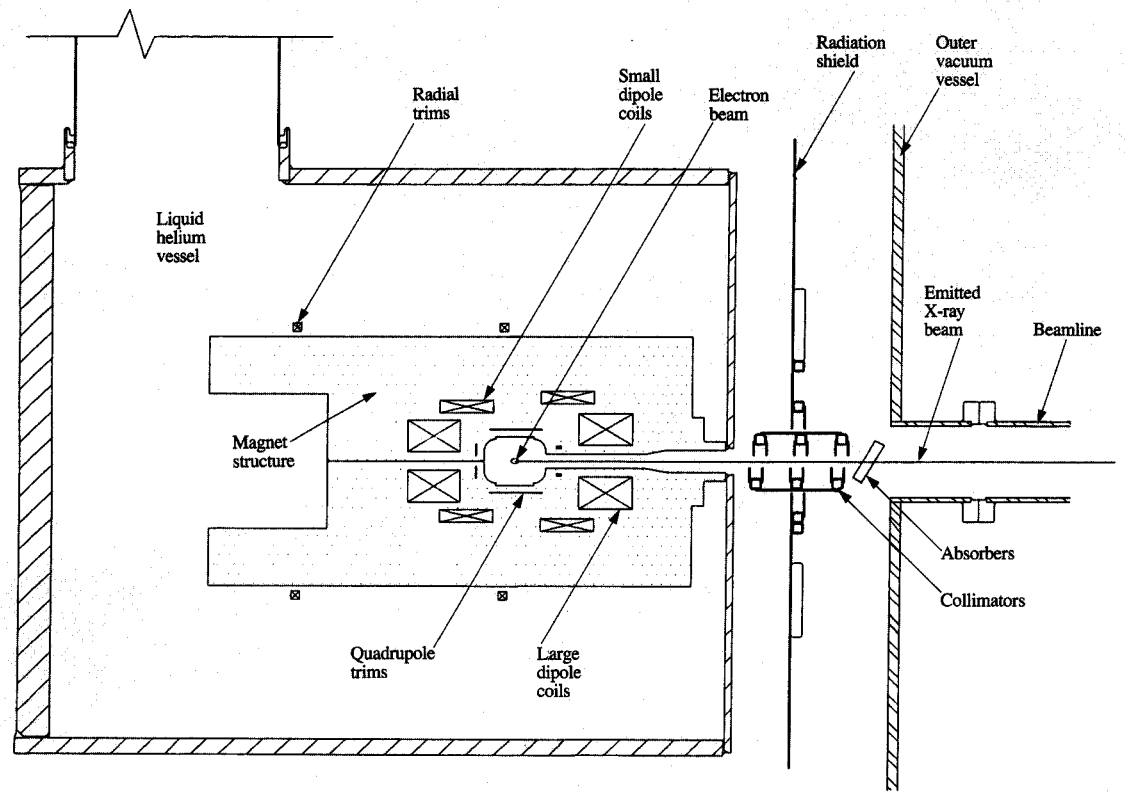

Figure 9

Simplified cross section of the superconducting dipole magnet, inside its liquid helium vessel, surrounded by a thermal radiation shield and contained within its vacuum vessel.

median plane), it has been possible to obtain the desired field shape with an accuracy of $\sim 5 \times 10^{-4}$.

The coils are wound from a flat "Rutherford cable" [13] consisting of 11 strands of copper/NbTi filamentary superconducting composite. Each wire contains 2000 filaments of NbTi alloy superconductor. The cable is insulated with a triple wrap of 25-mm Kapton™ film, but the coil is deliberately left porous to liquid helium for improved superconductor stability during ramping of the field. The four coils are mounted in a very substantial and accurately machined structure made from 304LN (nonmagnetic) stainless steel. Within this structure, they are preloaded to their working magnetic stress of ~ 15 MNm^{-2}. One of the design problems faced was the large magnetic force of ~140 tonnes exerted between the "outboard" coils located above and below the X-ray slot shown in Figure 9. Because the whole structure is at 4.3 K and the X-ray beam power is of the order of 10 kW, it is not possible to have any supporting material crossing this slot. Therefore, the forces must be taken by the surrounding structure, working as a kind of C-clamp. As noted earlier and shown in Figure 9, Helios uses a cold-bore vacuum system in which the surface immediately surrounding the electron beam is at 4.3 K.

Figure 10 shows the end windings of the coils, which are turned up and over the beam pipe. One advantage of this configuration is that, with careful attention to the detailed coil shape, one can achieve a good field profile throughout the end region. Other advantages of turned-up ends are that they allow the magnet to be rather short, they produce a relatively low peak field at the superconducting winding, and they leave a large clear vertical aperture for the beam; however, this shape of coil is quite difficult to fabricate.

Between the main coils and the beam aperture are the multipole trim coils; Figure 9 shows the quadrupole trims. They are wound from a single-wire filamentary superconducting composite wire of the same type as that used in the cable for the main coils. Quadrupole trims are

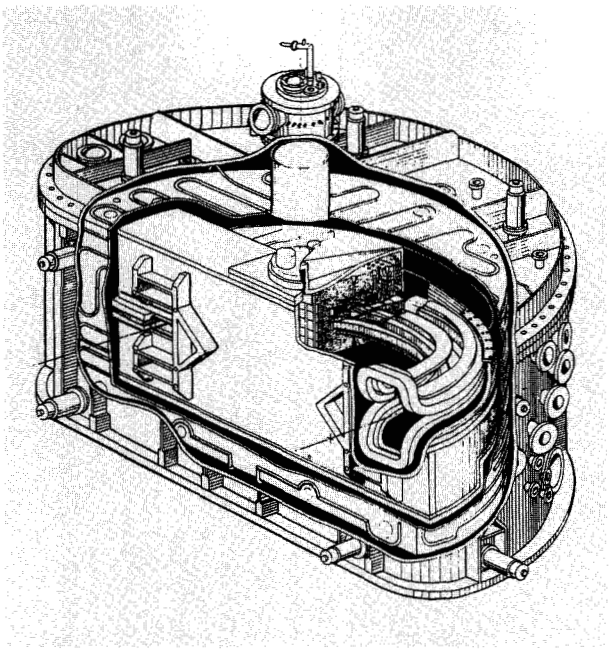

Figure 10

Cutaway view of the complete dipole magnet inside its liquid helium cryostat, showing the end windings of the superconducting coils.

located in the central region of the 180° arc and are used to change the gradient and hence the betatron tune of the ring. At each end of the dipole, the same cross section is occupied by the sextupole trims, which are used to correct the chromaticity of the ring. In addition, as shown in Figure 9, radial field trim windings are provided to compensate for any departure from vertical of the dipole field or any slight misalignment of the magnets when installed on the ring.

To intercept thermal radiation coming from the outer vacuum vessel, the liquid helium vessel is surrounded by a radiation shield cooled with liquid nitrogen. As shown in Figure 10, this is a stainless steel fabrication, cooled by an array of pipes welded to it. It is essential to leave a continuous slot along the midplane of this shield to permit the exit of X-rays from the beam. Figure 9 shows how this slot is made in the form of a collimator, so as to minimize the solid angle available for room-temperature radiation to shine back onto the helium vessel. In this way, the input of thermal radiation may be restricted to a few watts.

At the extreme right-hand side of Figure 9 is the outer vacuum vessel, which is penetrated by the 11 beam ports used to convey X-rays to the lithography lines or to diagnostic devices. At all other points around the arc, the X-rays are absorbed within the vacuum vessel by a water-cooled copper absorber, also shown in Figure 9. The magnet and radiation shield are suspended and located transversely within this vessel by titanium alloy support rods.

After completion of winding, and before assembling into its operational cryostat, each dipole magnet is tested at Oxford in a large tub-shaped cryostat of a type normally used for testing large medical imaging magnets; **Figure 11** sketches the general arrangement. In the course of this test, the magnetic field at all points around the 180° arc is measured using the "mouse" shown in **Figure 12.** The mouse carries a fixed array and a rotating array of Hall probes, which measure the field in the form of a Fourier expansion around a circle within the magnet aperture and perpendicular to the electron orbit:

$$B = \sum_{n=1}^{n=5} A_n r^n \cos n\theta, \tag{17}$$

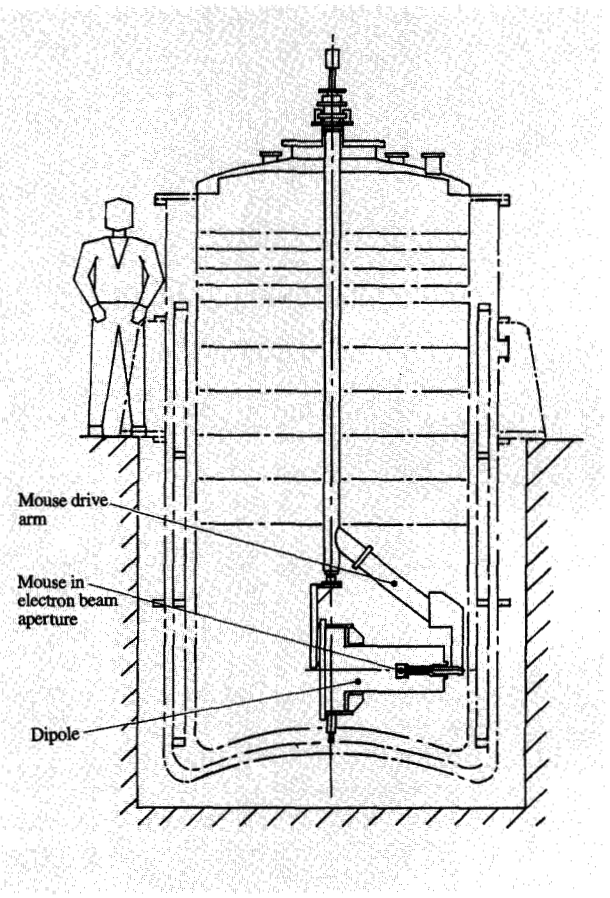

Figure 11

Measuring the dipole magnet field shape using a large open test cryostat. The mouse, within the dipole aperture, is driven along the electron orbit by the large rotary arm.

where r is the radial distance from orbit to measuring point and θ is the angle between the rotating array and the horizontal plane.

Results from this measurement are then fed into the Daresbury computer code ORBIT, which tracks many orbits of electrons around a ring in which the dipoles have the measured field characteristics. From these tracking studies, it is possible to predict the *dynamic aperture* of the ring. This aperture, which is determined by the magnetic field quality, defines the maximum stable oscillation of an electron from the equilibrium orbit. Electrons outside the dynamic aperture are lost because the field errors are too large to allow stable oscillations of this amplitude. Our criteria for acceptance of the field quality was that the dynamic aperture coming from these plots should be at least as great as the physical aperture. In other words, the whole physical aperture of the ring is available to store stable beam. Incidentally, it was found necessary for this work to modify the standard tracking routines, which were developed for use on large storage rings, in two important aspects [14, 15]. First, the frequently assumed approximation that the amplitude of the electron oscillation is small compared with the bending radius is not valid in compact rings. Second, another common approximation that the magnetic fields are "hard-edged" (i.e., the field is constant over a certain length and then falls to zero) does not apply to short high-field magnets.

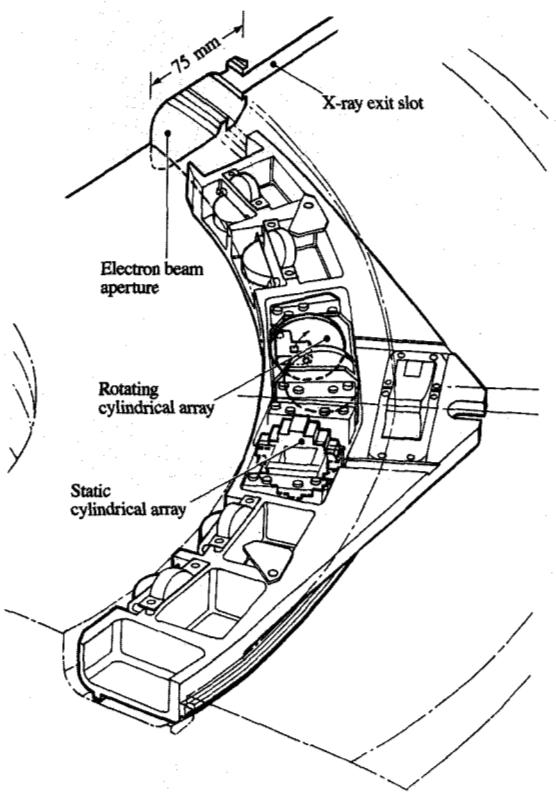

Figure 12

The field-measuring mouse, which follows the electron trajectory inside the dipole magnet aperture, measuring field quality as it goes.

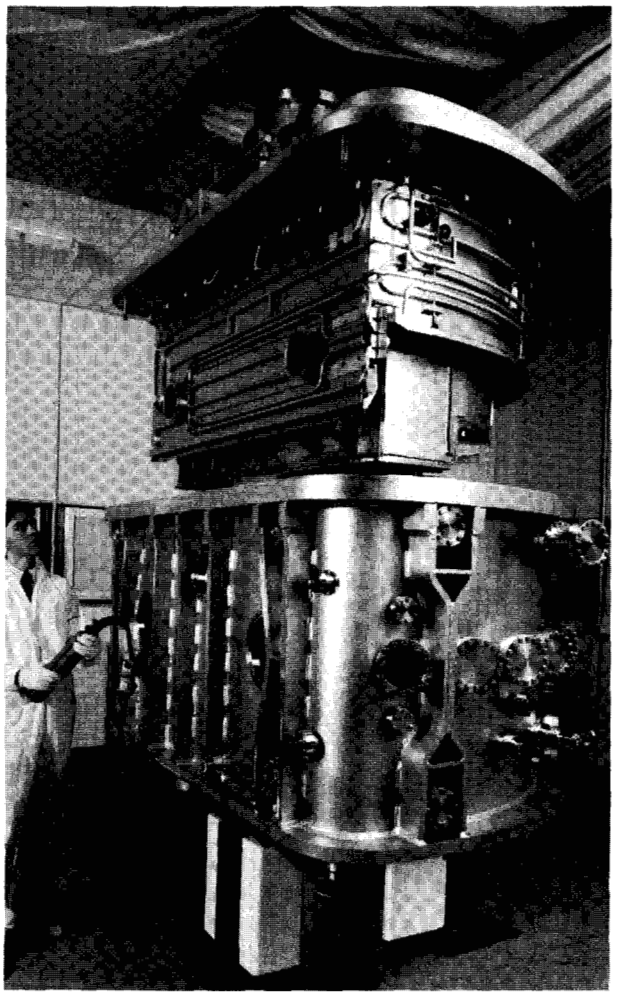

Figure 13

Assembling the dipole magnet, with thermal radiation shield, into its outer vacuum vessel.

After satisfactory completion of their magnetic tests, dipoles are welded into their helium vessels and very carefully checked for leaks. They are then subjected to a thorough UHV cleaning process before being assembled, with the radiation shields, into their vacuum vessel, as shown in **Figure 13**. Both dipoles are then integrated with the ring. After closure of the vacuum system, the dipole

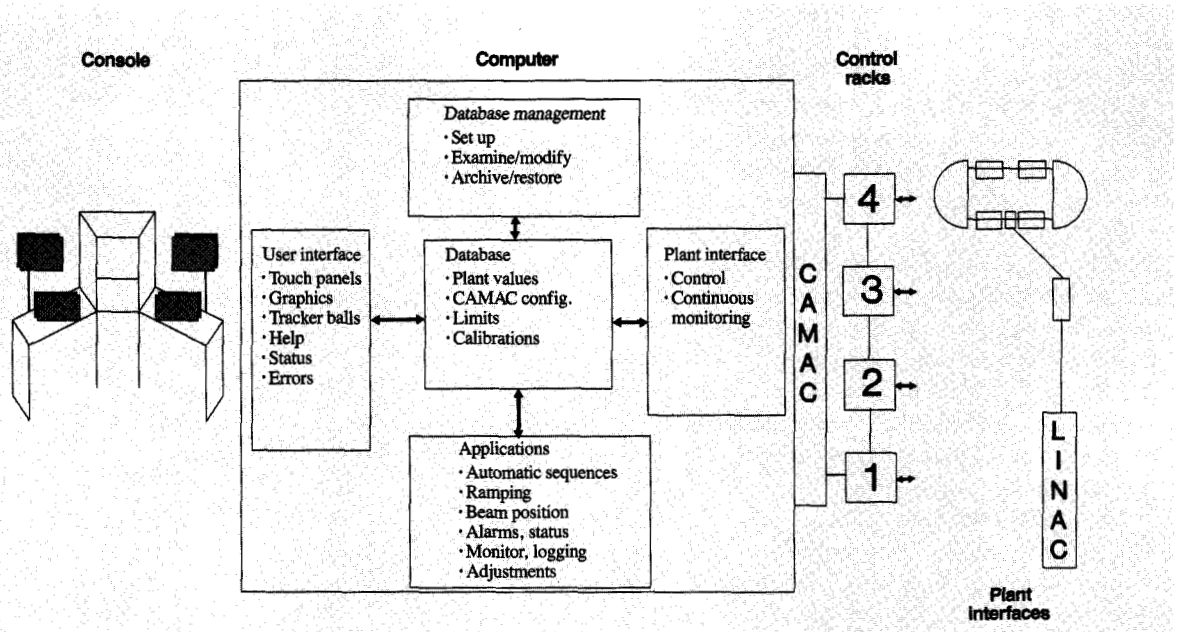

Figure 14

Layout of HECAMS control system hardware and schematic of the software.

and straight-section vacuum vessels are baked under vacuum to remove adsorbed gases. A total of six ion pumps, located in each straight section and in the dipole vessels, are then switched on, and the dipoles are cooled to ~4.3 K. As a result of this cooling, pressure in the dipole vessels falls below 10^{-10} torr, appreciably less than the average ring pressure cited in Table 2.

Cooling for the magnet is provided by a Sulzer TCF20 liquid helium refrigerator of ~100 W capacity, providing a good reserve of cooling power. As insurance against refrigerator failure, a buffer storage dewar of 3500 liters capacity is provided, sufficient for several days' operation if the refrigerator fails. Thus far, however, no extended refrigerator failures have occurred.

Controls and diagnostics

The Helios Control and Monitoring System (HECAMS) enables a single operator to control and monitor all functions of the ring, injector, and ancillary plant. To relieve the operator of routine tasks, it provides a set of automatic control sequences for routine operations. Specialized operations are available only to authorized operators, and parameter settings are limited to protect Helios from accidental misuse. For long-term trend analysis, HECAMS provides a log of all Helios parameters; for immediate retrospective fault analysis, it provides a short-term transient log.

Figure 14 shows a general layout of HECAMS [16], for which the software was developed by Oxford from an original suite of software written at the Stanford Linear Accelerator Center [17]. A database of some 800 signals, resident in a DEC Microvax computer, lies at the heart of the system. A CAMAC interface program passes control and monitoring information between this database and the hardware four times a second. Figure 14 shows how the hardware interface is divided among four control racks, which also contain the hard-wired interlocks for plant protection. Most plant items, such as magnet power supplies, pass information to HECAMS at a relatively low level, but the larger items, such as linac, have their own local intelligence.

The operator interface is via a touch panel and a display screen; two identical interfaces are provided for convenience during commissioning. For routine operation, extensive use is made of the automatic sequencing programs to relieve the operators of routine and repetitive tasks. One such sequence brings the linac to a state at which it is ready for injection; another brings the ring and transfer line to the same state. The main sequence, known as FILL, sets up the linac and transfer line, injects as

many pulses as needed to stack a prescribed current in the ring, ramps the magnets in synchronism, and controls the rf during the ramp, thus achieving stored beam at full energy without the need for manual intervention.

In addition to its many software functions, HECAMS incorporates a set of hard-wired circuits for fast control in real time, such as synchronizing the linac and kicker pulses. Another set of hard-wired circuits protects Helios and its ancillary plant from the consequences of faults, accidental misuse, overload, etc.

A variety of diagnostic devices are provided, principally to measure the location of the electron beam, but also to measure the tune of the beam and to detect signals from the beam in the time domain. The main devices, with locations as shown in **Figure 15**, are as follows:

- Beam position monitors (BPMs), each comprising an array of four capacitive buttons located around the beam pipe, with circuitry to measure the *XY* coordinates of the beam by addition and subtraction. Four units are located at each end of the ring straights, and three are in the injection transfer line.
- Scintillator screens (S) made of caesium iodide, which may be inserted at two locations in the transfer line and one in the ring, for a (destructive) measurement of beam position and visualization of its profile.
- Toroids (T) for measuring linac current.
- Tickler striplines for inducing very small transverse oscillations in the stored beam which may then be picked up by the BPMs. In this way, the betatron tunes may be measured as a resonance in the frequency response.
- Wide-band pickups for detecting time structure in the beam.
- A toroidal current transformer (TCM) for accurately measuring stored current.
- Synchrotron light monitors (SLMs) consisting of an optical system and TV camera, for measuring the position, shape, and stability of the beam in each dipole.

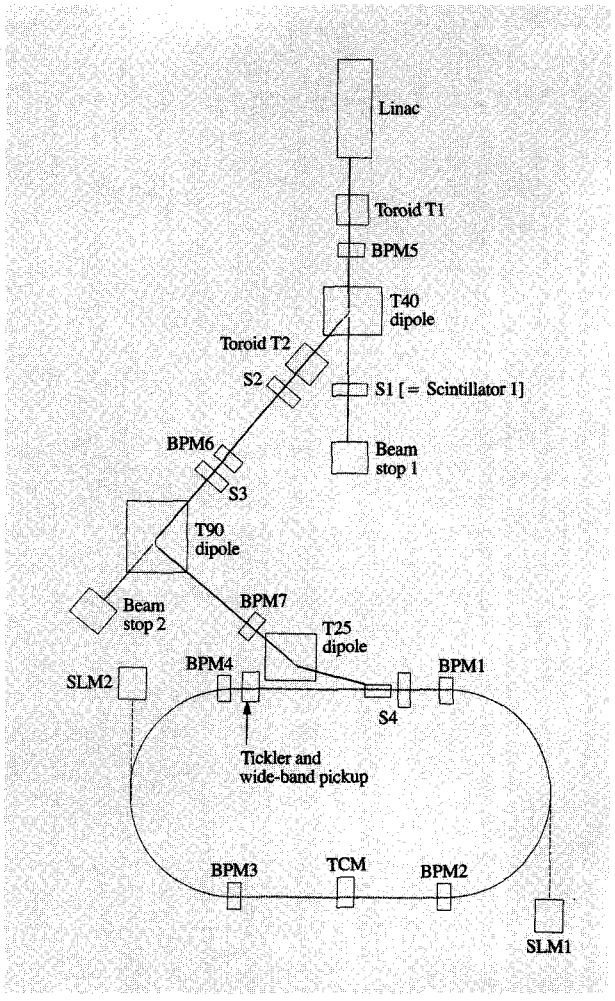

Figure 15

Locations of diagnostics in the injection line and storage ring.

Signals to and from most diagnostics are connected to HECAMS so that they may be controlled and logged in the usual way.

Commissioning and operation at Oxford

After completion of the assembly work, Helios 1 was moved into the radiation-shielded enclosure at Oxford for testing with electron beams. The linac had already been commissioned and was able to produce pulses of ~20 mA, within the required ±0.5% energy band and with a pulse length of ~120 ns. When it has been established that all ring systems are functioning correctly, the first task is to align the injected beam so that it enters the ring correctly through the septum magnet. This alignment is carried out by adjusting several steering trim magnets in the injection transfer line in the light of information from the various BPMs and the scintillator screen immediately downstream from the septum. When an accurate beam path has been established, the scintillator is retracted so that beam can pass through the first dipole. By using the radial field trims in dipole 1 together with BPMs in the downstream straight, an accurate path is then established through dipole 1 and, subsequently, through dipole 2. The injected beam is then able to coast around the ring freely, with a lifetime of about 450 μs, determined by energy losses via synchrotron radiation in the dipoles.

Next, the rf cavity is switched on, so that synchrotron radiation losses are replaced and the beam can circulate continuously at injection energy. Under these steady-state conditions, injection performance may be optimized by

Figure 16

Helios 1 inside its shipping crate being loaded onto a road vehicle for transportation from Oxford to East Fishkill.

adjusting the kicker amplitude and timing and the septum amplitude.

Betatron tune of the stored beam is now measured, using the tickler electrodes and BPMs. A suitable operating tune is selected, comfortably removed from any potentially disruptive resonance, by adjusting the quadrupoles. Similarly, the chromaticity is measured and adjusted to be zero by using the sextupoles.

One may now begin ramping to full energy by increasing all the magnetic fields in unison. This is initially done in stages, stopping at the end of each stage to measure and, if necessary, adjust the tune, chromaticity, and closed-orbit position. At each stage, HECAMS stores the readjusted magnet settings and then interpolates between them to synthesize a smoothed and corrected ramp function. By using the optimized ramp, beam may now be accelerated continuously to full energy, ramping the fields in ~3 min.

At the conclusion of commissioning in Oxford, 540 mA had been accumulated in the ring at injection energy and 100 mA had been ramped to full energy. This performance, in fulfilment of the IBM stage 1 specification, served to indicate that the ring design was fundamentally sound and that achievement of the full specification could be safely deferred until the final optimization on site at East Fishkill. The ring was therefore shut down for minor improvements and modifications prior to shipment. The most important of these improvements was to replace the ion pumps and make detailed modifications to the vacuum system. The excellent lifetimes subsequently achieved for stored beams at ALF were to show the benefits of these modifications.

Transportation, installation, and commissioning at ALF

By virtue of its rigid stainless steel base frame, Helios can be transported easily around the factory on air flotation pads. All control cabling, utilities, etc. are brought to a common connection point on this frame so that they may be quickly and easily uncoupled. During the closing phases of work at Oxford, an advance site installation party had started work at ALF to install duplicate cabling so that the ring could be quickly connected up on arrival.

Figure 16 shows Helios 1 being loaded onto the road vehicle at the beginning of its journey to East Fishkill. A rigid steel cage has been bolted to the baseframe and serves the dual function of lifting cradle and shipping crate. Shock-absorbing mountings and the use of an air-ride truck served to restrict accelerations during the trip to <2 g. Within two weeks of leaving Oxford, Helios 1 had crossed the Atlantic via the roll-on roll-off ferry and was being moved into position at ALF.

A stored beam of 50 mA was established just two months after arrival on site at ALF, and the full specification of 200 mA at full energy was exceeded some two months later [18]. Details of subsequent operations are presented in [9] and [19].

Conclusions

Electron storage rings are the only known source of X-rays with sufficient continuous power for the needs of production X-ray lithography. The high fields available from superconducting magnets enable rings to be built which are much smaller than conventional rings, for the same output wavelengths and power. They also allow the ring to be injected at lower energy. Compact size has obvious benefits in minimizing the space required in the wafer fabrication facility but, even more importantly, it enables the ring to be transported intact from factory to user site as a fully tested unit. The relatively rapid installation and achievement of full specification on site at ALF have shown the value of this feature.

References

1. E. E. Koch, D. E. Eastman, and Y. Farge, *Handbook on Synchrotron Radiation*, G. V. Marr, Ed., Elsevier, New York, 1987, Ch. 1.
2. G. Margaritondo, *Introduction to Synchrotron Radiation*, Oxford University Press, Oxford, England, 1988.
3. J. J. Livingood, *Principles of Cyclic Particle Accelerators*, Van Nostrand Reinhold, New York, 1988.
4. E. D. Courant and H. S. Snyder, "Theory of Alternating Gradient Synchrotron," *Ann. Phys.* **3**, No. 1, 1–48 (1958).
5. D. Seeger, "Resist Materials and Processes for X-Ray Lithography," *IBM J. Res. Develop.* **37**, No. 3, 435 (1993, this issue).
6. R. P. Haelbich, J. P. Silverman, W. D. Grobman, J. R. Maldonado, and J. M. Warlaumont, "Design and Performance of an X-Ray Lithography Beam Line at a Storage Ring," *J. Vac. Sci. Technol. B* **1**, No. 4, 1262 (1983).
7. M. Sands, "The Physics of Electron Storage Rings," *Report No. SLAC-121*, Stanford Linear Accelerator Center, Stanford, CA, 1979.
8. M. N. Wilson, "Compact Synchrotron X-Ray Sources," *Proceedings of the 2nd European Accelerator Conference*, Nice, France, June 1990, p. 295.
9. Chas Archie, "Performance of the IBM Synchrotron X-Ray Source for Lithography," *IBM J. Res. Develop.* **37**, No. 3, 373 (1993, this issue).
10. P. Letellier, G. Meyrand, C. Perraudin, A. Setty, D. T. Tran, D. Tonc, V. C. Kempson, and J. A. Uythoven, "Commissioning the 200 MeV Injector linac for the Oxford Instruments IBM Synchrotron Light Source," *Proceedings of the 1989 IEEE Particle Accelerator Conference*, Chicago, 1989, p. 1082.
11. R. J. Anderson, E. P. Gibbons, and S. T. Perry, "Operation of the Helios 1 Compact Synchrotron RF System," *Proceedings of the Third European Particle Accelerator Conference, EPAC 92*, Editions Frontières, Gif sur Yvette, France, 1992, p. 1191.
12. R. P. Walker, "Calculation of the Touschek Lifetime in Electron Storage Rings," *Proceedings of the 1987 IEEE Particle Accelerator Conference*, Washington, DC, 1987, p. 491.
13. M. N. Wilson, *Superconducting Magnets*, Oxford University Press, Oxford, England, 1983.
14. E. J. N. Wilson, "Small Ring Lattice Problems," *Proceedings of the CERN Accelerator School*, Uppsala, Sweden, September 18–29, 1989; *CERN Report 90-04*, April 24, 1990.
15. C. N. Archie and J. A. Uythoven, "Tracking Studies for the Oxford Instruments Compact Electron Synchrotron," *Conference Record, IEEE Particle Accelerator Conference*, 1991, p. 1594.
16. A. R. Jorden, G. M. Howes, S. Woodward, and M. C. Wilson, "Control System for a Compact Synchrotron," *Nucl. Instrum. & Meth. A* **293**, 70 (1990).
17. S. Howry, T. Gromme, A. King, and M. Sullenberger, "A Portable Database Driven Control System for SPEAR," *Proceedings of the 1985 Particle Accelerator Conference*, Vancouver, BC; *IEEE Trans. Nucl. Sci.* **NS-32**, No. 5, 2104 (1985).
18. C. N. Archie, J. I. Granlund, R. W. Hill, K. W. Kukkonen, J. A. Leavey, L. G. Lesoine, J. M. Oberschmidt, A. E. Palumbo, C. Wasik, M. Q. Barton, J. P. Silverman, J. M. Warlaumont, A. D. Wilson, R. J. Anderson, N. C. Crosland, A. R. Jorden, V. C. Kempson, J. Schouten, A. I. C. Smith, M. C. Townsend, J. Uythoven, M. C. Wilson, M. N. Wilson, D. E. Andrews, R. Palmer, R. Webber, and A. J. Weger, "Installation and Early Operating Experience with the Helios Compact X-Ray Source," presented at the 36th Annual Symposium on Electron, Ion, and Photon Beams, Orlando, FL, May 1992; *J. Vac. Sci. Technol. B* **10**, No. 6, 3224 (1992).
19. D. E. Andrews and C. N. Archie, "Early Experience with the Helios Compact X-Ray Source," *Proceedings of the International Conference on Microcircuit Engineering*, Erlangen, Germany, September 1992, to be published.

Received January 11, 1993; accepted for publication March 15, 1993

Martin N. Wilson *Oxford Instruments Ltd., Accelerator Technology Group, Osney Mead, Oxford OX2 0DX, England.* Dr. Wilson is General Manager of the Accelerator Technology Group at Oxford Instruments. He joined Oxford in 1983 to work on compact superconducting synchrotrons and was also responsible for the early work at Oxford on superconducting cyclotrons. Prior to joining Oxford, he worked at the Rutherford Laboratory, primarily on applied superconductivity, but also on pulsed high-field magnets and energy systems. In the year 1986–1987 he was a visiting scientist at the Magnet Laboratory of MIT. Dr. Wilson is the author of more than 60 papers on applied superconductivity and the book *Superconducting Magnets* (Oxford University Press, 1983). In 1989 he was awarded, jointly with A. Tollestrupp, the American Institute of Physics Robert R. Wilson Prize for work on superconducting accelerators. He is a graduate of Manchester University and is a Fellow of the Institute of Physics and a member of the IEEE.

Alistair I. C. Smith *Oxford Instruments Ltd., Accelerator Technology Group, Osney Mead, Oxford OX2 0DX, England.* Dr. Smith graduated with a B.Sc. in applied physics from Heriot-Watt University, Edinburgh, in 1969 and the following year received an M.Sc. in applied solid state physics from Brighton Polytechnic. Three years of research in the field of surface analysis led to the award of a Ph.D. in physics in 1973. He then took a position with Gillette R & D Labs in Reading, England, working initially on ion source development and ion implantation; subsequently, as head of the surface analysis group, he was responsible for ESCA and Auger analysis of the surface modification of steels. In 1976 he moved to VG Scientific Ltd., the largest European manufacturer of UHV and surface analysis equipment. After a period in sales and marketing, in 1981 he was appointed Managing Director of the Electron Microscope Division–VG Microscopes. When this company was subsequently merged with the surface analysis operations, he assumed the position of Managing Director of the combined operation in 1984. Dr. Smith moved to Oxford Instruments in 1988 as Managing Director of the Semiconductor Systems Division, responsible for the Oxford Group's activities in both plasma and ion beam equipment and the Accelerator Technology Group, of which the Helios program forms a part.

V. C. Kempson *Oxford Instruments Ltd., Accelerator Technology Group, Osney Mead, Oxford OX2 0DX, England.* Mr. Kempson is Manager of the Systems Department in the Accelerator Technology Group. He received his B.Sc. in applied physics from Lanchester College in 1979 and is a member of the Institute of Physics. He spent many years in the accelerator group at the Rutherford Laboratory working on 3D magnet design, pulsed magnet design, and accelerator test and commissioning on the ISIS pulsed neutron source. He joined Oxford Instruments in 1985 in a special projects group. Mr. Kempson is now Project Manager for Helios 2.

Martin C. Townsend *Oxford Instruments Ltd., Accelerator Technology Group, Osney Mead, Oxford OX2 0DX, England.* Mr. Townsend is Manager of the Production Department, responsible for all mechanical/electrical manufacture, assembly, and test within the Accelerator Technology Group. He earned Higher National Certificates in mechanical engineering (1983) and electrical engineering (1990) from Oxford Polytechnic and joined Oxford Instruments Ltd. as Technician Apprentice in August 1979. For ten years Mr. Townsend has worked in the manufacture, test, and installation of cryogenic and magnet systems. During his six years within the Accelerator Technology Group, Mr. Townsend has developed ultrahigh vacuum systems and superconducting bending magnets.

Joseph C. Schouten *Oxford Instruments Ltd., Accelerator Technology Group, Osney Mead, Oxford OX2 0DX, England.* Dr. Schouten studied applied physics and engineering at the Technical University of Delft, The Netherlands, receiving his Diploma in engineering in 1976. He continued further research at the Technical University of Eindhoven, where he obtained a Ph.D. in technical sciences in 1981. After being a Research Fellow of the Royal Norwegian Institute for Scientific and Technical Research, he joined the Imperial College of Science and Technology in London to design and build the first European magnetic monopole detector. In 1985 Dr. Schouten joined Oxford Instruments as a Senior Engineer, becoming Product Manager in 1988 at their Research Instruments Company. In 1991 he moved to the Accelerator Technology Group as Engineering Manager of the Dipole Section. Apart from working on the dipoles for the Helios superconducting synchrotron, he is the Project Manager for the Cebaf cold iron quadrupoles which are currently under construction. Dr. Schouten is a chartered physicist, a member of the Institute of Physics, and a member of the Dutch Physical Society; he holds a Professional Diploma in management.

Robert J. Anderson *Oxford Instruments Ltd., Accelerator Technology Group, Osney Mead, Oxford OX2 0DX, England.* Mr. Anderson received a B.Sc. in electronic engineering from Birmingham University in 1973 and an M.Sc. in information and systems engineering in 1975. After four years with the Ministry of Defence and two years with the Racal Redac computer-aided design company, he joined the joint European Torus project (JET) in 1982. At JET he worked in the RF Heating Division on teams responsible for the installation of 30 MW of ion cyclotron resonance heating and subsequently a 12-MW lower hybrid resonance current drive system. He joined Oxford Instruments to build Helios in 1987. Mr. Anderson is a member of the Institute of Electrical and Electronics Engineers and a chartered engineer.

A. R. Jorden *Oxford Instruments Ltd., Accelerator Technology Group, Osney Mead, Oxford OX2 0DX, England.* Mr. Jorden graduated from the Imperial College of Science and Technology, London, in 1972 with a first-class honors degree in physics. After three years of research and development in electronics with the Plessey Radar Research Centre, he spent ten years developing advanced photon detectors as astronomical imaging systems at the Royal Greenwich Observatory. Since joining Oxford Instruments in 1986, he has been the team leader responsible for developing the controls and beam diagnostics for the Helios synchrotron. Mr. Jorden is a chartered physicist and a SPIE member.

Victor P. Suller *SERC Laboratory, Warrington, Cheshire WA4 4AD, England.* Mr. Suller is head of the Synchrotron Radiation Accelerator Division at the UK's synchrotron light facility, a 2-GeV high-brilliance electron storage ring. He received his B.Sc. in physics at Birmingham University in 1964, with an M.Sc. in 1965. After a year doing research on metallic thin films for integrated circuit applications at Ferranti Research, he joined Daresbury Laboratory to become an accelerator physicist in 1966. Thereafter, he contributed to the development of the Nina 5-GeV electron synchrotron, which was used for high-energy particle physics research until 1977. In 1972 he focused attention on accelerators for synchrotron light production, taking responsibility for the design of the 2-GeV SRS in 1974 and its commissioning in 1980.
Mr. Suller has also contributed to the design of the European Synchrotron Radiation Facility since 1977. In 1984 he directed the collaboration between Daresbury Laboratory and Oxford Instruments Ltd. which culminated in the design of the Helios compact source.

Michael W. Poole *SERC Daresbury Laboratory, Synchrotron Radiation Accelerator Division, Warrington, Cheshire WA4 4AD, England.* Mr. Poole is a physics graduate of the University of Liverpool; he subsequently joined the beam physics team on the Nina high-energy electron synchrotron at Daresbury. He has extensive experience in the development of electromagnets for accelerators and was responsible for the design, construction, and testing of all magnet systems for both the booster synchrotron and storage ring of the SRS national light source from 1974 to 1980. Mr. Poole is now Head of Accelerator Physics on the SRS and was also Acting Head of the RF Group for two years. In addition to his work at Daresbury, he served on the ESRF Machine Sub-Group from 1979 to 1982 and since 1984 has been an accelerator physics adviser to Oxford Instruments on the Helios project. In 1983 he designed the first UK undulator, which has since become a user facility on the SRS. He has had a long involvement in free-electron laser development, both in the UK and as an international advisor to the Felix project in the Netherlands, and he has been a member of the International FEL Executive Committee for many years. In 1986 Mr. Poole was Chairman of the 8th International FEL Conference. Recently, he has worked on design plans for new UK light sources and has also been project leader on the superconducting wiggler project. He has given many invited talks on accelerators and free-electron lasers, and is a CERN Accelerator School Lecturer. In 1992 he received an SERC Individual Merit Promotion for his work.